The Astrophysical Journal, 612:L69–L72, 2004 September 1

FREE-FREE RADIO EMISSION FROM YOUNG STELLAR OBJECTS

Hsien Shang,[1] Susana Lizano,[2] Al Glassgold,[3] and Frank Shu[4]

Received 2004 May 8; accepted 2004 July 20; published 2004 August 5

ABSTRACT

We calculate the centimeter wavelength free-free emission of the jets of young stellar objects (YSOs) with the *X*-wind model enhanced by a variety of physical processes. Using parameters characteristic of a Class I YSO with a mass-loss rate of $\sim 10^{-6}\ M_\odot\ \mathrm{yr}^{-1}$, we obtain a 3.6 cm map and a spectral index that compare well with high spatial resolution observations of L1551 IRS 5. Models with lower mass-loss rates, appropriate for Class II YSOs with revealed optical jets, produce radio jets that are too weak to be detected at current sensitivity levels. In addition to demonstrating the consistency of the density distribution of the *X*-wind model with observations, we are able to obtain information on the processes that heat and ionize the inner jet, i.e., X-ray ionization and shock heating and ionization.

Subject headings: ISM: Herbig-Haro objects — ISM: jets and outflows — radiation mechanisms: thermal — radio continuum: stars — stars: winds, outflows

1. INTRODUCTION

Free-free radio emission has been detected in more than 100 outflows (e.g., Eislöffel et al. 2000) from both high- and low-luminosity young stellar objects (YSOs). The emission from low-luminosity YSOs is generally weak, typically a half to a few millijanskys. The jetlike structure in well-observed (nearby and luminous) sources shows that the radio emission is collimated on a scale smaller than 10 AU. Thus, high angular resolution maps of radio jets probe deep into the launch region and present a significant challenge for theoretical models of YSO outflows.

Thermal bremsstrahlung emission at centimeter wavelengths has a flat or positive spectral power index p (flux density $S_\nu \propto \nu^p$). The classic example of an unresolved, constant velocity, fully ionized, isothermal, spherical wind has $p = 0.6$. Reynolds (1986) showed that $p < 0.6$ occurs for an unresolved, partially opaque flow whose cross section grows more slowly than its length. The index can vary from $p = 2$ for totally opaque emission to $p = -0.1$ for totally transparent emission. Observers have usually interpreted radio data with Reynolds' model, obtaining the spectral index from total flux measurements at several wavelengths. With the development of the *X*-wind model (Shu et al. 1994, 2000), including physical properties calculated from first principles (Shang et al. 2002, hereafter SGSL), a more detailed analysis is now possible.

The production of millijansky radio emission (see Anglada 1996 for a review) has long been a problem for the theory of jets in low-mass YSOs. Previous workers agreed that stellar radiation produced too little ionization to account for the observations (e.g., Rodríguez et al. 1989). Opinion has shifted on the role of shock-produced UV radiation (e.g., Curiel et al. 1987). González & Cantó (2002) recently obtained thermal radio emission at the millijansky level by modeling periodically driven shocks in a spherical wind. In the calculations of SGSL, a main source of ionization is X-ray radiation, an essentially universal property of YSOs (Feigelson & Montmerle 1999). Most of the heating comes from dissipation of the mechanical energy of the wind in turbulence and shocks. A suggestion from the current work is that UV radiation from the same shocks may play a role in the ionization structure of radio jets.

Generating collimated jets is an essential task for theoretical models of the outflows from YSOs. The *X*-wind approach of SGSL has been successful in producing the observational properties of the forbidden lines of S II and O I that are a diagnostic of the temperature and electron density of the optical jets of revealed sources. Observations of radio jets probe embedded sources that are too heavily extincted to be visible at optical wavelengths. Even when both are observed, the radio emission is at the base of the optical jet. Because of the penetrating power of centimeter waves, radio jets are useful in probing the underlying driving mechanism of jets. The present application of the *X*-wind model to radio continuum emission is timely in the context of developing capabilities for improved high spatial resolution radio observations. It should also help us to discriminate between different theoretical approaches, e.g., between disk winds (reviewed by Königl & Pudritz 2000) and *X*-winds.

In this Letter we consider the well-observed outflow source L1551 IRS 5, variously referred to in the literature as a Class 0 or Class I YSO, and model the radio jet observed at 3.6 cm by Rodríguez et al. (2003, hereafter R03) as free-free emission from an *X*-wind. The parameters of the model are partly chosen on the basis of our previous discussion of the optical jets of revealed sources. The choice of model parameters is important since only Class 0 and Class I YSOs have mass-loss rates large enough to produce radio jets detectable with current sensitivity. In the following, we describe our model in more detail (§ 2), then present results (§ 3), and conclude with a brief summary (§ 4).

2. THEORETICAL BACKGROUND

The basic parameters of the SGSL thermal-chemical-dynamical model are the stellar mass M_*, radius R_*, bolometric luminosity L_*, magnetic dipole moment μ_*, X-ray luminosity L_X, and the disk mass accretion rate $\dot{M}_D$, which gives the wind mass-loss rate $\dot{M}_w = f\dot{M}_D$, with $f \approx 0.25$. We adopt typical values of the radius $R_x = 0.923(\mu_*^4/G\dot{M}_*M_D^2)^{1/7}$ of the inner-disk edge (Ostriker & Shu 1995) that range from $R_x \approx 3R_*$ for protostars ($\dot{M}_w \sim 10^{-6}\ M_\odot\ \mathrm{yr}^{-1}$) to $R_x \approx 5R_*$ for T Tauri stars ($\dot{M}_w \lesssim 1 \times 10^{-8}\ M_\odot\ \mathrm{yr}^{-1}$). For a low-mass Class 0 or Class I

[1] Institute of Astronomy and Astrophysics, Academia Sinica, P.O. Box 23-141, Taipei 106, Taiwan; shang@asiaa.sinica.edu.tw.

[2] Centro de Radioastronomía y Astrofísica, UNAM, Apartado Postal 72-3 (Xangari), 58089 Morelia, Michoacán, Mexico; s.lizano@astrosmo.unam.mx.

[3] Department of Astronomy, University of California, 601 Campbell Hall, Berkeley, CA 94720-3411; aglassgold@astro.berkeley.edu.

[4] National Tsing Hua University, 101, Section 2, Kuang Fu Road, Hsinchu 30013, Taiwan; presid@mx.nthu.edu.tw.

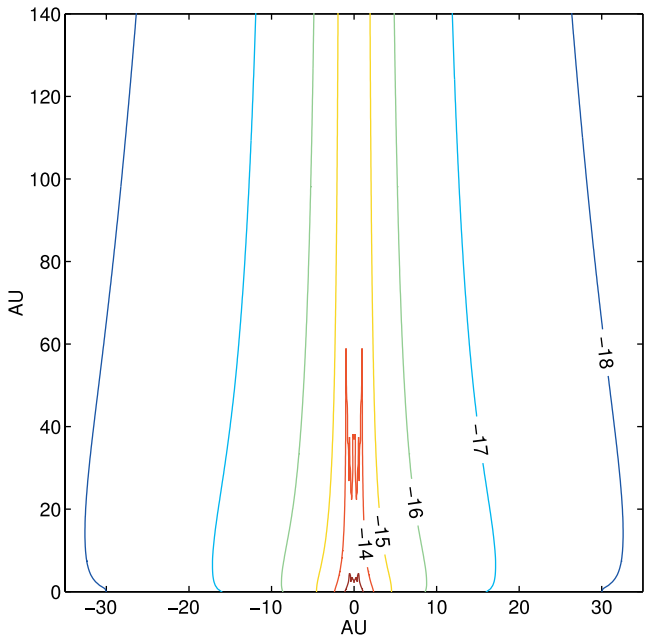

FIG. 1.—Free-free intensity contours (in units of ergs cm^{-2} s^{-1} sr^{-1}) for the *X*-wind model using parameters scaled up from the SGSL ratio, $L_X/\dot{M}_w = 2 \times 10^{13}$ ergs g^{-1}: $\dot{M}_w = 10^{-6}\ M_\odot$ yr^{-1}, $L_X = 1.3 \times 10^{33}$ ergs s^{-1}, $\alpha = 0.005$, and $\beta = 0$.

source responsible for the radio jets studied in this Letter, we choose $M_* = 0.5\ M_\odot$ and $R_* = 3\ R_\odot$.

SGSL noted that X-rays affect the thermal and ionization structure of the *X*-wind through the combination $L_X/\dot{M}_w$. This follows from the well-known fact that the X-ray ionization rate ζ_X enters rate equations (including the hydrodynamic heat equation) through the ratio ζ_X/n_H, where n_H is the volume density of hydrogen nuclei. This scaling with the X-ray ionization parameter breaks down when other ionization processes are competitive. In discussing the forbidden lines of T Tauri stars, we used $L_X/\dot{M}_w = 2 \times 10^{13}$ ergs g^{-1}, based on $\dot{M}_w = 3 \times 10^{-8}\ M_\odot$ yr^{-1} and $L_X = 4 \times 10^{31}$ ergs s^{-1}. The quantity $L_X/\dot{M}_w$ can be interpreted as the *average* efficiency for converting accretion power into X-rays at radius R_x: $L_X/\dot{M}_w = \epsilon_X GM_*/fR_x$ (Shu et al. 1997). For example, GM_*/fR_x is 4×10^{14} ergs g^{-1} for the model T Tauri star in SGSL, which implies $\epsilon_X \sim 0.05$. For $\dot{M}_w = 10^{-6}\ M_\odot$ yr^{-1}, appropriate for the Class 0/Class I source L1551 IRS 5, the corresponding value of L_X is 1.3×10^{33} ergs s^{-1}. Such a large X-ray luminosity has only been observed in rare protostellar flares (Grosso et al. 1997; Feigelson & Montmerle 1999; Tsuboi et al. 2000). We begin with such models, but we move later to models that assume smaller X-ray luminosities, compensating for the decrease with enhanced mechanical sources of heating and ionization.

Among the microphysical processes for a magnetocentrifugally driven wind included by SGSL are ionization of hydrogen from the $n = 1$ and $n = 2$ levels via Lyman and Balmer continuum photons emitted by both the accretion funnel hot spots and the star itself. Bremsstrahlung cooling was omitted since it is small compared with line cooling, but it is included here for completeness. Molecular hydrogen is not considered. The main synthesis pathway for H_2 formation via the H^- ion is ineffective because collisional dissociation is so strong at the high temperatures (>8000 K) of jets. Furthermore, H_2 emission has not been detected from the jet proper of fast outflows (Davis et al. 2002, 2001).

We adopt the SGSL phenomenological expression for the volumetric mechanical heating rate:

$$\Gamma_{\rm mech} = \alpha\rho\frac{v^3}{s}, \tag{1}$$

where ρ and v are the local gas density and flow velocity, respectively, in a frame at rest with respect to the star, and s is the distance a fluid element has traveled along a streamline in the flow. The phenomenological parameter $\alpha \geq 0$ reflects the magnitude of the disturbances in the flow, possibly magnetic in origin, that lead to the dissipation of mechanical energy into heat. We anticipate $\alpha \ll 1$ so that only a small fraction of the mechanical energy is dissipated by shocks or magnetoturbulent cascades. Small α is also required for consistency with the cold flow assumption in *X*-wind theory. Modeling of the forbidden lines led to values of α in the range 0.002–0.005. For the radio jet work discussed below, values somewhat larger, perhaps by a factor of 2, are needed.

The shock waves encompassed in equation (1) can also produce UV radiation in the Balmer and Lyman continua that ionize as well as heat the gas. In the same spirit as equation (1), we can represent this ionization rate per unit volume by the formula

$$P_e = \beta n_H v/s, \tag{2}$$

where β is a phenomenological shock-ionization parameter.

To calculate the free-free emission in the resulting *X*-wind, we use the equation of radiative transfer for the steady monochromatic intensity for each line of sight. The optical depth of the thermal free-free radio emission scales with the square of the electron density profile, and the resultant intensity is weakly dependent on temperature and sensitive to the electron density. In contrast, the forbidden-line emission is sensitive to both the temperature and the electron density.

3. RESULTS

We focus on the thermal radio jets observed by R03 in L1551 IRS 5, located in the Taurus molecular cloud at a distance of 140 pc. L1551 IRS 5 has a bolometric luminosity of 30–40 $L_\odot$ and an accretion rate of $\sim 10^{-5}\ M_\odot$ yr^{-1} (Adams et al. 1987), consistent with the wind mass-loss rate of $\sim 2 \times 10^{-6}\ M_\odot$ yr^{-1} obtained from H I observations (Giovanardi et al. 2000). Very Large Array (VLA) observations at 7 mm reveal two circumstellar disks of a binary system (Rodríguez et al. 1998). Using the VLA with the Pie Town antenna at 3.6 cm and an angular resolution of about 0.″1 (14 AU), R03 mapped the radio jets of the binary at the center of the larger scale (~1″) jets observed at optical and NIR wavelengths (Fridlund & Liseau 1998; Itoh et al. 2000). The total 3.6 cm flux density of the source is ~4 mJy, with about half (1.7 mJy) coming from the compact cores (both sides) of the two jets. This system provides the best available data for comparison with theory at the present time.

Starting from the work of SGSL, we try to construct a steady jet model that can produce the observed 3.6 cm flux density of ~1.2 mJy associated with the stronger core of the south radio jet and counterjet in L1551 IRS 5 (R03). We first adopt $\alpha = 0.005$, $\beta = 0$ (no shock-wave ionization), and $L_X/\dot{M}_w = 2 \times 10^{13}$ ergs g^{-1} (same ratio as SGSL), along with $\dot{M}_w = 10^{-6}\ M_\odot$ yr^{-1}. Using a very small pixel size (~3 mas in the transverse direction), Figure 1 shows the resulting intensity of the jet seen edge-on (by assuming reflection symmetry about the midplane for the counterjet). The intensity contours range from 10^{-18} to

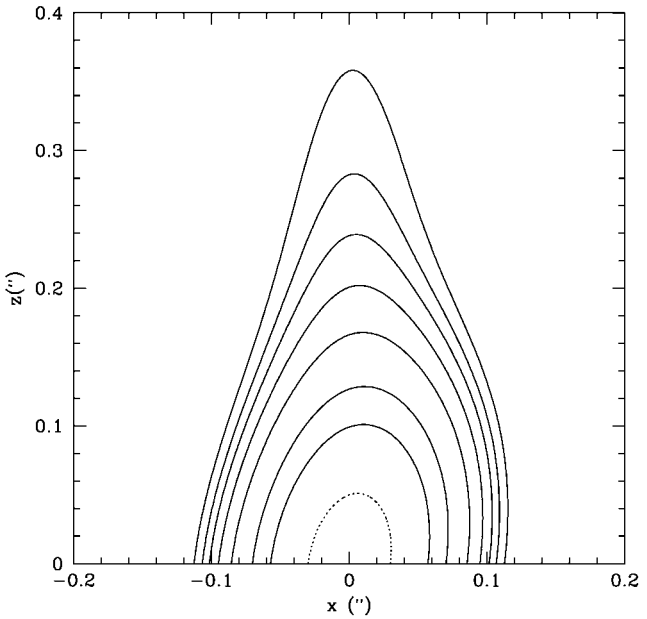

FIG. 2.—Convolved intensity at 3.6 cm for the model of Fig. 1 using a beam of 0.″12 × 0.″18, inclined at 20° with respect to the jet axis. The solid contours are 80, 100, 120, 150, 200, 300, and 400 μJy beam^{-1}. The dotted innermost contour corresponds to 600 μJy beam^{-1}. The half-length of the jet core is 0.″36, and the flux (jet and counterjet) is 1.6 mJy.

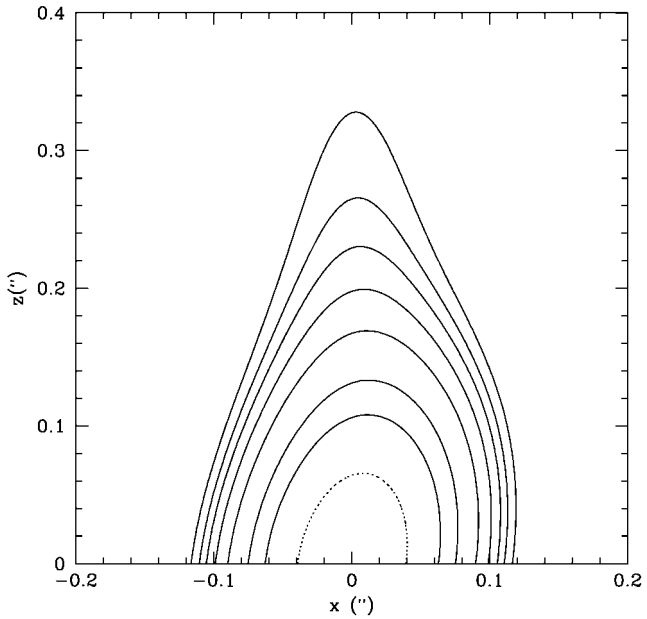

FIG. 3.—Convolved map at 3.6 cm for a model with reduced $L_X = 1.3 \times 10^{32}$ ergs s^{-1} and $\alpha = \beta = 0.007$. The solid and dotted contours correspond to the same levels as in Fig. 2. This model also produces a flux of 1.6 mJy. The half-length of jet core is 0.″33.

10^{-13} ergs cm^{-2} s^{-1} sr^{-1} and exhibit cylindrical collimation of the electron density. They also show a cusplike behavior near the vertical axis due to the presence of a hollow core in the model. The ionization fraction is of order a few percent, and the temperature on the axis is $\sim 10^4$ K. Within 20 AU of the *z*-axis, the electron density is in the range 10^4–10^6 cm^{-3}. Closer to the star, within a few AU, it reaches $\geq 10^7$ cm^{-3}. This high-density region poses interesting challenges for future high angular resolution observations.

A map of the convolved intensity at 3.6 cm of the model in Figure 1 is shown in Figure 2. The model was convolved with a 0.″12 × 0.″18 beam, whose position angle is 20° (north to east), as in the observations of R03. This convolution with an inclined beam produces an observed asymmetry with respect to the jet axis. The solid contours correspond to the seven highest contours in Figure 1 of R03, and the 80 μJy beam^{-1} contour defines the outer extent of the jet cores. The half-length of the model jet core is $\sim$0.″36, and the total flux (doubled to account for jet and counterjet) is 1.6 mJy, somewhat larger than the 1.2 mJy of the observations, primarily because of the existence of an extra innermost contour (*dotted curve*). Apart from this minor discrepancy, Figure 2 fits nicely both the spatial variation of the flux density and the resolved length of the observed jet core. The observations do not resolve the jet in the direction perpendicular to the jet axis. We make no attempt to compare additional lower level contours given by R03 because they suggest external disturbances that might arise through the interaction of the separate winds from the binary source. Overall, the contours in Figures 1 and 2 show the central peaking and elongation found in the observations of R03. The model in Figure 1 has a 6 cm flux of 1.4 mJy, which implies a spectral index $p = 0.3$. This prediction could be tested by simultaneous 0.″1 resolution observations at 3.6 and 6 cm to avoid problems with variability.

In Table 1 we summarize the model results as a function of mass loss at 3.6, 6, and 0.7 cm for the case $\alpha = 0.005$, $\beta = 0$, and $L_X/\dot{M}_w = 2 \times 10^{13}$ ergs g^{-1}. For mass-loss rates lower than $3 \times 10^{-7}\ M_\odot$ yr^{-1}, $S_\nu \propto \nu^{-0.1}$, characteristic of optically thin free-free emission. For higher mass-loss rates, the spectra turn over and gradually steepen to $p \sim 0.3$ for $\dot{M}_w \approx 10^{-6}\ M_\odot$ yr^{-1}. Table 1 shows that in order to detect radio jets with the VLA with good sensitivity in its highest resolution configuration, the YSO must have $\dot{M}_w > 3 \times 10^{-7}\ M_\odot$ yr^{-1}.

Although the model in Figures 1 and 2 reproduces the size and overall spatial variation of the observed radio jet in L1551, it assumes a very large X-ray luminosity, $L_X = 1.3 \times 10^{33}$ ergs s^{-1}. The ionization produced close in by the X-rays is carried outward in the slowly recombining flow. To explore the trade-off between decreasing L_X and increasing α, we varied these two parameters over a range of acceptable values. We found that good solutions for L1551 IRS 5 exist for L_X smaller than that used in Figure 1 for α in the still modest range of 0.005–0.01, provided we allow for the possibility of a nonzero value for β (i.e., shock-induced UV ionization). Figure 3 shows

TABLE 1

TOTAL MODEL FLUX DENSITIES FOR $L_X/\dot{M}_w = 2 \times 10^{13}$ ergs g^{-1}, $\alpha = 0.005$, AND A DISTANCE OF 140 pc

PARAMETER	$\dot{M}_w$			
	$3 \times 10^{-8}\ M_\odot$ yr^{-1}	$1 \times 10^{-7}\ M_\odot$ yr^{-1}	$3 \times 10^{-7}\ M_\odot$ yr^{-1}	$1 \times 10^{-6}\ M_\odot$ yr^{-1}
$S_{6\,\mathrm{cm}}$ (5 GHz) (mJy)	1.7×10^{-2}	0.076	0.30	1.4
$S_{3.6\,\mathrm{cm}}$ (8.3 GHz) (mJy)	1.6×10^{-2}	0.073	0.30	1.6
$S_{7\,\mathrm{mm}}$ (43 GHz) (mJy)	1.3×10^{-2}	0.060	0.25	2.1
Spectral index p	−0.1	−0.1	0.0	0.3

a convolved radio jet image for a choice of L_X that is 10 times smaller than in Figure 2, but with $\alpha = \beta = 0.007$. The total flux from this model is 1.6 mJy. The radio image of Figure 3 is very similar to Figure 2, including an extra innermost (dotted) contour, and could just as well represent the present state of observations for L1551.

The phenomenological heating of equation (1) was introduced by SGSL in their modeling of the optical jets in active T Tauri stars. Both equations (1) and (2) have the nice property that their spatial variation is scale-free. But one must question whether this formulation really applies without modification at the small distances $s \rightarrow 0$ probed by radio jets. A generalization of the spatial dependence in the shock heating and ionization laws adopted in these equations from $1/s$ to $1/(s + s_0)$ can eliminate the unwanted innermost (dotted) contours in Figures 2 and 3. Figure 4 shows an example with $\alpha = \beta = 0.01$, $s_0 = 2$ AU, and $L_X = 1.3 \times 10^{32}$ ergs s^{-1}. The total flux produced in this model is 1.3 mJy and gives a size about 0.″30 for either side of the jet. A similar modification of the model in Figure 2 with a choice of $s_0 = 1$ AU produces approximately the same size and total flux. A length scale s_0 of a few AU, interior to which there are only weak shocks or none at all, could represent the periodicity length in the type of pulsed model advocated by González & Cantó (2002), modified for jetlike geometries.

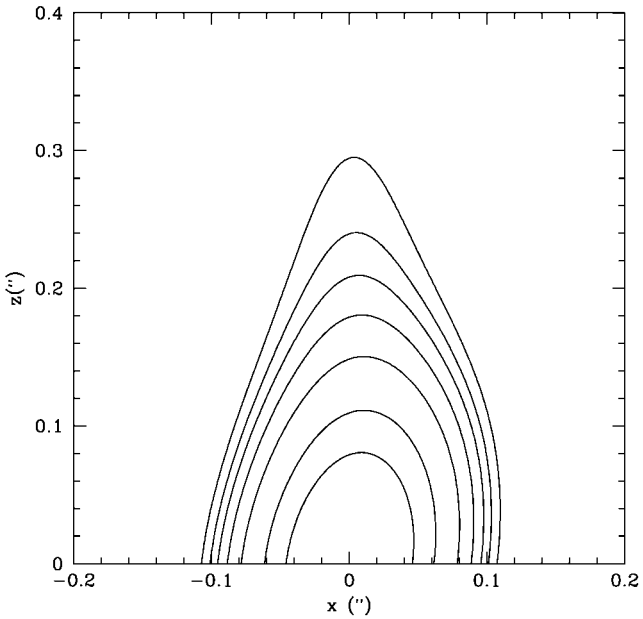

FIG. 4.—Convolved map at 3.6 cm for a similar model as in Fig. 3, with $\alpha = \beta = 0.01$ and $s_0 = 2$ AU. The same solid contours are plotted, but the inner dotted contour has disappeared. This model has a total flux (jet and counterjet) of 1.3 mJy and a half-length of 0.″3.

4. DISCUSSION AND INTERPRETATION

We have calculated radio continuum images and spectra for the free-free emission of the *X*-wind model heated and ionized by the processes discussed by SGSL and extended to include shock ionization. Several general properties—total fluxes, spectral indices, and sizes—agree with the observations compiled by Anglada (1996, Table 2). More specifically, the maps in Figures 2, 3, and 4 compare quite well with the observations of the southern jet core in L1551 IRS 5 (R03).

Our calculations indicate that the radio flux from YSOs with mass-loss rates much below $3 \times 10^{-7}\ M_\odot$ yr^{-1} is too weak to be detected with current sensitivity. The strongest centimeter-continuum jet sources among low-mass YSOs, e.g., L1551, HL Tau, DG Tau B, and HH 111, do have bright optical jets on larger scales. Instrumental improvements that would allow the simultaneous measurements of radio and optical radiation from the same source would help to better constrain the parameters of the theory. Enough data already exist to associate the detectable radio jets with younger and embedded low-mass YSOs that have strong molecular outflows (Rodríguez & Reipurth 1994). It is gratifying that the theoretical framework provided by the *X*-wind model for interpreting the radio and optical data allows this semiquantitative relationship to be established for YSO jet sources with ages and spectral energy distributions that span the range from Class 0 (embedded protostars) to Class II (classical T Tauri stars).

We acknowledge fruitful discussions with L. Rodríguez, P. Ho, W. J. Welch, P. D'Alessio, and G. Anglada. We also thank the anonymous referee for helpful suggestions. Support has been received from these grants: Theoretical Institute for Advanced Research in Astrophysics, Academia Sinica, and National Tsing Hua University, NSC92-2112-M-007-051 and NSC92-2112-M-001-062 in Taiwan; DGAPA/UNAM IN104202 and CONACyT 40091 for S. L.; and NSF grant AST-0097978 for A. G.

REFERENCES

Adams, F. C., Lada, C. J., & Shu, F. H. 1987, ApJ, 312, 788
Anglada, G. 1996, in ASP Conf. Ser. 93, Radio Emission from the Stars and the Sun, ed. A. R. Taylor & J. M. Paredes (San Francisco: ASP), 3
Curiel, S., Cantó, J., & Rodríguez, L. F. 1987, Rev. Mex. AA, 14, 595
Davis, C. J., Ray, T. P., Desroches, L., & Aspin, C. 2001, MNRAS, 326, 524
Davis, C. J., Stern, L., Ray, T. P., & Chrysostomou, A. 2002, A&A, 382, 1021
Eislöffel, J., Mundt, R., Ray, T. P., & Rodríguez, L. F. 2000, in Protostars and Planets IV, ed. V. Mannings, A. P. Boss, & S. S. Russell (Tucson: Univ. Arizona Press), 815
Feigelson, E. D., & Montmerle, T. 1999, ARA&A, 37, 363
Fridlund, C. V. M., & Liseau, R. 1998, ApJ, 499, L75
Giovanardi, C., Rodríguez, L. F., Lizano, S., & Cantó, J. 2000, ApJ, 538, 728
González, R. F., & Cantó, J. 2002, ApJ, 580, 459
Grosso, N., Montmerle, T., Feigelson, E. D., Andre, P., Casanova, S., & Gregorio-Hetem, J. 1997, Nature, 387, 56
Itoh, Y., et al. 2000, PASJ, 52, 81
Königl, A., & Pudritz, R. E. 2000, in Protostars and Planets IV, ed. V. Mannings, A. P. Boss, & S. S. Russell (Tucson: Univ. Arizona Press), 759
Ostriker, E. C., & Shu, F. H. 1995, ApJ, 447, 813
Reynolds, S. P. 1986, ApJ, 304, 713
Rodríguez, L. F., Myers, P. C., Cruz-González, I., & Terebey, S. 1989, ApJ, 347, 461
Rodríguez, L. F., Porras, A., Claussen, M. J., Curiel, S., Wilner, D. J., & Ho, P. T. P. 2003, ApJ, 586, L137 (R03)
Rodríguez, L. F., et al. 1998, Nature, 395, 355
Rodríguez, L. F., & Reipurth, B. 1994, A&A, 281, 882
Shang, H., Glassgold, A. E., Shu, F. H., & Lizano, S. 2002, ApJ, 564, 853 (SGSL)
Shu, F., Najita, J., Ostriker, E., Wilkin, F., Ruden, S., & Lizano, S. 1994, ApJ, 429, 781
Shu, F. H., Najita, J. R., Shang, H., & Li, Z.-Y. 2000, in Protostars and Planets IV, ed. V. Mannings, A. P. Boss, & S. S. Russell (Tucson: Univ. Arizona Press), 789
Shu, F. H., Shang, H., Glassgold, A. E., & Lee, T. 1997, Science, 277, 1475
Tsuboi, Y., Imanishi, K., Koyama, K., Grosso, N., & Montmerle, T. 2000, ApJ, 532, 1089